Bioorganic Chemistry 90 (2019) 103056

Contents lists available at ScienceDirect

Bioorganic Chemistry

journal homepage: www.elsevier.com/locate/bioorg

Synthesis, anti-diabetic evaluation and molecular docking studies of 4-(1-aryl-1*H*-1, 2, 3-triazol-4-yl)-1,4-dihydropyridine derivatives as novel 11-β hydroxysteroid dehydrogenase-1 (11β-HSD1) inhibitors

Praveenkumar E.[a], Nirmala Gurrapu[a], Prashanth Kumar Kolluri[a], Vishwanadham Yerragunta[b], Bharathi Reddy Kunduru[c], Subhashini N.J.P.[a,*]

[a] Department of Chemistry, University College of Science, Osmania University, Hyderabad, Telangana 500 007, India
[b] Bio-organic & Medicinal Chemistry Research Division, Vishnu Institute of Pharmaceutical Education and Research (VIPER), Narsapur, Medak, Telangana 502 313, India
[c] Department of Genetics and Biotechnology, University College of Science, Osmania University, Hyderabad, Telangana 500 007, India

ARTICLE INFO

Keywords:
11-BetaHydroxysteroid dehydrogenase-1(11β-HSD1) inhibitors 1, 4-dihydropyridine
1,2,3–Triazole
Diabetic agents and molecular docking studies

ABSTRACT

11-Beta-Hydroxysteroid dehydrogenase-1(11β-HSD1) inhibitors are one of the emerging classes of molecules to fight against diabetic complications. A novel series of 4-(1-substituted-1*H*-1,2,3-triazol-4-yl)-1,4-dihydropyridine derivatives were synthesized and evaluated for their anti-diabetic activity. Two compounds showed anti-diabetic activity very effectively. To clarify the mechanism of action of these compounds, the most potent compounds (5g and 5h) of the synthesized analogs were further studied by testing its 11-Beta Hydroxysteroid dehydrogenase-1 inhibitory activity through *in vitro* enzymatic experiments. The results showed that the 11β-HSD1 inhibitory activity of compounds 5g and 5h was stable and efficient. Molecular docking studies revealed compounds 5g (−9.758) and 5h (−8.495) to have a stable binding patterns to the human 11-Beta-Hydroxysteroid dehydrogenase-1.

1. Introduction

Adipose tissue is an important source in governing energy equity and glucose homeostasis. As an energy repository, adipose tissue responds to the body's metabolic signaling by controlling lipid depot and mobilization. Adipocytes liberate free fatty acid (FFA) as a nutrient source when glucose levels are decreasing, whereas they store ample energy as triglycerides in an energy excess environment. Insulin resistance can uplift the FFA limits, and excessive FFA leads to deterioration of metabolic state by stimulating liver glucose output and by impeding glucose uptake by peripheral tissues and the generation of a reactive oxygen system (ROS), which, in turn, provoke insulin resistance [1]. Adipose tissue is an important portion of the endocrine system, which liberates many adipokines, such as leptin, GBP-28, Nicotinamide phosphoribosyltransferase, (NAmPRTase), omentin, and adipose tissue-specific secretary factor (ADSF), to control glucose homeostasis and whole body insulin sensitivity. Thus, adipocyte dysfunctioning may lead to pathogenic characteristics of obesity and metabolic disorders such as type 2 diabetes [2]. Glucocorticoid is an antagonizing hormone of insulin that triggers hepatic glucose production and inhibits insulin-dependent glucose uptake in peripheral tissues such as adipose tissue and skeletal muscle. Excess glucocorticoid in Cushing's syndrome, develops obesity and many clinical complications correlated with insulin resistance, such as type 2 diabetes, hypertension and dyslipidemia [3]. The target tissue activity of glucocorticoid is measured not only by considering its circulating status but also by the local glucocorticoid stimulation, which is controlled by 11β-hydroxysteroid dehydrogenase type 1 (11β-HSD1) and 11β-HSD2. 11β-HSD1, which is widely expressed in the liver, adipose tissue, gonads, and brain, and potentiate the glucocorticoid activation (cortisol in human and corticosterone in rodents) from inoperative 11-keto steroids (cortisone in human and 11-dehydrocorticosterone in rodents). This process multiplies locally centralized glucocorticoid action, whereas 11β-HSD2 is widely expressed in aldosterone-sensitive target tissues such as kidney, colon, salivary glands and placenta and also catalyzes counter reactions [4]. High glucocorticoid levels in adipocytes reduce insulin-dependent glucose uptake, accelerates FFA secretion and alters adipokine profiles, thus develop in insulin resistance [5]. Therefore, 11β-HSD1 is expected to play a critical role in governing glucose and lipid metabolism in adipose tissue. Many preclinical studies have been reported to illustrate the role of 11β-HSD1 in acquiring insulin resistance and the development of obesity [6]. Mice studies have been reported where the

* Corresponding author.
E-mail address: njsubhashini@osmania.ac.in (N.J.P. Subhashini).

https://doi.org/10.1016/j.bioorg.2019.103056
Received 11 February 2019; Received in revised form 29 April 2019; Accepted 6 June 2019
Available online 11 June 2019

adipose-specific overexpression of 11β-HSD1, displayed increased levels of corticosterone in adipose tissue and triggered insulin resistance, accumulated centric obesity, hyperlipidemia, and other features of metabolism-related disorders [7] whereas liver-specific overexpression of 11β-HSD1 in mice, led to development of mild insulin resistance and dyslipidemia [8]. 11β-HSD1 knockout mice displayed effective and improved glucose tolerance, an increased HDL level, and stability in weight fluctuation during a high-fat diet [9–11]. On another hand, overexpression of 11β-HSD2 in adipose tissue of mice resulted in the inactivation of glucocorticoid which led to a drastic drop in food intake and efficient glucose tolerance and high insulin sensitivity during the consumption of a high-fat diet [12]. Many studies on humans have reported two to three-fold increases of 11β-HSD1 activity in the adipose tissue of obese individuals, as a result of predominant 11β-HSD1 expression that has been positively correlated with the degree of obesity [13,14]. Based on the above findings, type 2 diabetes or metabolic disorders could possibly be effectively treated by specifically blocking adipose tissue expressed 11β-HSD1. 1, 4-dihydropyridines and their derivatives are one of the significant classes of medicinally and pharmacologically important molecules that occupy a major portion of angina and hypertension therapeutic modalities, such as nifedipine and felodipine [15], nicardipine [16], and amlodipine [17]. These molecules have been shown [18,19,20] that their pharmacological action is associated with voltage-dependent L-type calcium channel binding which in turn decreases the passage of Ca^{2+} ions in to the cytoplasm of the cell. This leads to relaxation of smooth muscles and lowering of the blood pressure. Another molecular mechanism that has been evaluated for their activity depends on elevated Nitric Oxide (NO) release from the intact endothelium [21]. 1, 4-Dihydropyridines have also been reported as anti-neoplastic [22], neurotropic [23], antiplatelet glycoprotein inhibitors [24], bronchodilating [25], and anti-diabetic agents [26]. In this study, taking into consideration the 11β-hydroxysteroid dehydrogenase-1 enzyme flexibility and dynamic properties, we designed a new series of 4-(1-aryl-1*H*-1, 2, 3-triazol-4-yl)-1,4-dihydropyridine derivatives from proven 11β-hydroxysteroid dehydrogenase-1 inhibitors [27]. The synthesized compounds were subjected to docking studies towards the human 11β-HSD1 enzyme to evaluate their affinity and binding interaction in the active site. The compounds were evaluated *in-vitro* and the most potent inhibitors from this novel series were assessed in further *in-vivo* studies for their ability to inhibit 11β-HSD1 associated diabetes mellitus (see Fig. 1).

2. Results and discussion

2.1. Chemistry

The synthetic route to the desired diethyl 4-(4-(1-(3-acetylphenyl)-1H-1, 2, 3-triazole-4yl) methoxy) phenyl)-2,6-dimethyl-1,4-dihydropyridine-3,5-dicarboxylates (5a-l) are summarized in Scheme 1. The 1, 4-dihydropyridine core nucleus of was constructed from commercially available compounds. The synthesis was started with the propargylation of 4-hydroxy benzaldehyde **(1)** using propargyl bromide to yield 4-[(prop-2-yn-1-yl)oxy]benzaldehyde **(2)** this was reacted with various aryl azides **(3a-f)** at the terminal alkyne position to provide compounds (**4a-f)** containing the 1,2,3-triazole ring of 4-hydroxybenzaldehydes, The final reactions involved the condensation of ethyl acetoacetate or methyl acetoacetate in presence of ammonium acetate with in presence of ethanol and the 1, 2, 3-triazole ring of 4-hydroxy benzaldehyde compounds (**4a-f)** under the microwave irradiation afforded targeted compounds (**5a-l) (**Scheme 1) Microwave irradiation afforded excellent yields short reaction times and environmental friendly conditions (see Table 1).

All compounds were characterized by ^{1}H NMR and ^{13}C NMR Spectres (supplementary data).

2.2. Anti-diabetic activity

Compounds 5a-l were screened for anti-diabetic activity and molecular docking studies were performed to evaluate enzyme inhibition using Schrodinger suite (see Table 4). The details of these studies are recorded in Tables 2 and 3.

2.2.1. In vitro anti-diabetic study

All the synthetic 4-(1-aryl-1*H*-1,2,3-triazol-4-yl)-1,4-dihydropyridine derivatives (5a-l) were evaluated for their *in vitro* inhibitory activity of the α-glucosidase enzyme by the method described by Nickavar and Yousefian, 2009, using Baker's yeast α-glucosidase enzyme. This microplate assay offers convenience, speed, and reproducibility. The alpha-glucosidase inhibitory activity was determined by quantifying the release of *p*-nitro phenol from *p*-nitro phenyl-D-glucopyranose. The released *p*-nitro phenol yields a yellow color when the stopping reagent, glycine (pH 10) is added. The results were summarized in Table 2. A relatively higher proportion of compounds showed a differential degree of α-glucosidase inhibitory activity with IC_{50} values between 72.71 and 283.41 μM when compared with acarbose standard (IC_{50} = 395.17 μM). Though all molecules of the series showed good inhibitory activity against the enzyme, compounds 5 g, 5 h, and 5i showed the best inhibitory activity among the series, with IC_{50} values 72.71 ± 1.09, 73.83 ± 1.17, and 85.96 ± 1.84 μM respectively. Alpha-glucosidase inhibitory activity of 4-(1-aryl-1*H*-1, 2, 3-triazol-4-yl)-1,4-dihydropyridine derivatives was analyzed and is shown in table 2. The activity of 5 g, 5 h and 5i were showed the best inhibiton compared to acarbose (98.7% @517.37 μM), having % inhibitions of 98.3 (@ 139.78 μM), 97.5 (@ (145.71 μM) and 96.8 (@ 159.87 μM), respectively (see Table 5).

2.2.2. In-vitro 11β-hydroxysteroid dehydrogenase assay:

Based on earlier studies, the enzymatic inhibitory activity of 5 g and 5 h against 11β -HSD1 was measured by scintillation proximity assay (SPA) using microsomes containing 11β-HSD1. From *in vitro* 11β -HSD1 Inhibitory studies performed for derivative molecules 5 g, 5 h, and 5i, 5 g and 5 h showed decreased activity of 11β-HSD1, and they showed (Graph 1) significant synchrony with 18α-glycyrrhetinic acid.

2.2.3. In-silico molecular docking studies

Considering the results obtained from *In-vitro* inhibition of 11β-Hydroxysteroid dehydrogenase activity, it was thought worthy to perform molecular docking studies by substantiating the *in-silico* studies. Comparative docking studies of 11βeta-hydroxysteroid dehydrogenase-binding protein with compounds 5a-l and against standard Rosiglitasone exhibited good affinity. Molecules 5a-l were analyzed by molecular docking studies by using Schrödinger's (2015) molecular docking software. Molecules were constructed in a maestro build interface panel and developed by Lig prep 2.3. module by applying default parameters. The crystal structures of Murine **11-beta-hydroxysteroid dehydrogenase 1**: 11βeta from an established structure (PDB ID: 1Y5M) file was downloaded from the protein data bank (www.rcsb.org). The protein was prepared using protein the preparation wizard of Schrödinger's molecular docking software. In this target preparation, all water molecules were removed and hydrogen atoms were added to the target. The grid was generated around the active functional site of the protein by selecting the co-crystallized ligand. Receptor Van-der Waals scaling for nonpolar atoms was kept at 0.9. Ligands with low energy conformers were selected and docked into the generated grid using extra precision (XP) docking mode. The dock score and energy of each ligand was quantified in silico for their molecular interactions with the receptor grid.

The empirical binding positions between 5g and 11-Beta-hydroxysteroid dehydrogenase 1 are reported in Fig. 2. Molecule 5 g adopted an "L-shaped" conformation in the binding pocket of the 11β -HSD1. The triazolyl 1, 4-dihydropyridine group of 5g was approached the hydrophobic pocket, which was surrounded by residual amino acids, Phe-157, Phe-310, and Phe-311, while the acetyl moiety of 5g was

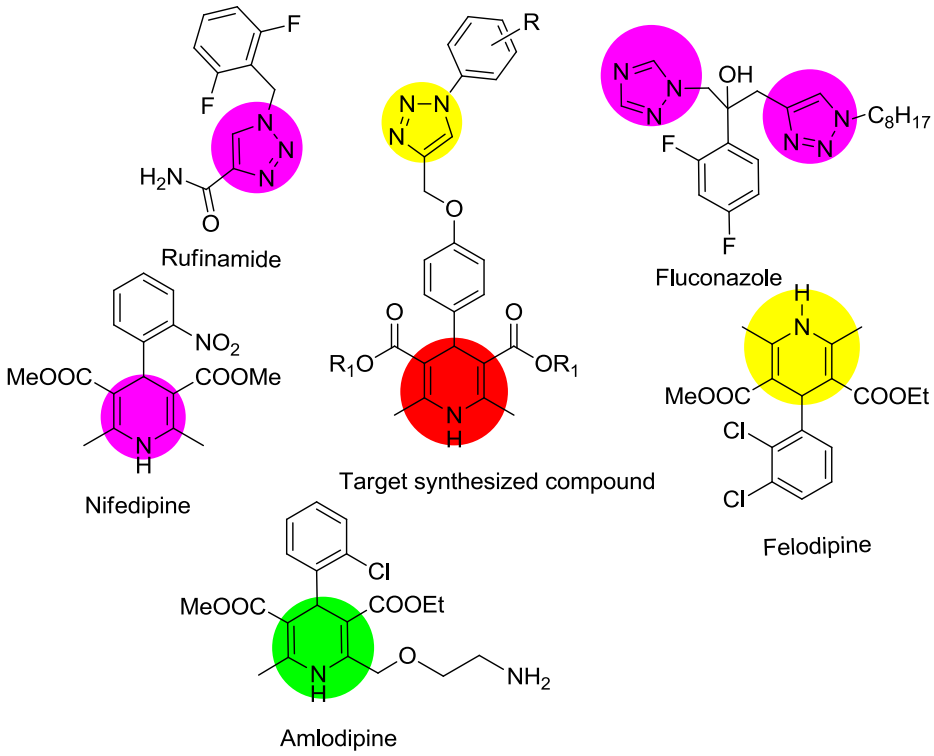

Fig. 1. Biologically active drugs having 1, 4-dihydropyridines and 1, 2, 3-triazoles.

expanded into the hydrophobic pocket, consisting of residues Phe-157, Phe-177 and Phe-300, forming a stable hydrophobic binding pattern. Comprehensive docking analysis revealed that the triazole group of **5g** developed a CH-π interaction with the Phe-300 residue. On the other hand, Cation-π interactions were identified between 5g and Lys-155, Arg-312 and Arg-439 residues. In addition, compound 5g developed anion-π interactions with Glu-276 and Asp-349 residues respectively. All these interactions supported compound 5g in the binding site of the 11β -HSD1. In order to identify the activity of 5h against 11β-HSD1, compound 5h was then docked to the binding pocket of 11β -HSD1. More stable empirical binding pose between 5h and 11β -HSD1 is shown in Fig. 3. The molecular interactions between 5h and 11β -HSD1 were similar to those identified between 5g and 11β -HSD1 with the only difference being the 1,4-dihydropyridine group of 5h established π-π stacking interactions with His-239 and Phe-157 residues, which were not developed by 5g, this makes 5 h marginally less active than 5 g against 11β -HSD1 (Figs. 2 & 3). On the other hand, the in silico

Table 1
Physical data of synthesized compounds (**5a-l**).

Entry	R^1	R^2	R^3	R^4	M.p's (°C)	Product (Yield %)
5a	H	H	H	$-C_2H_5$	165–167	87
5b	H	H	H	$-CH_3$	156–158	85
5c	H	OCH_3	H	$-C_2H_5$	148–150	89
5d	H	OCH_3	H	$-CH_3$	140–142	87
5e	H	H	CH_3	$-C_2H_5$	142–144	84
5f	H	H	CH_3	$-CH_3$	135–137	83
5g	H	$COCH_3$	H	$-C_2H_5$	162–164	85
5h	H	$COCH_3$	H	$-CH_3$	151–153	84
5i	H	Cl	H	$-C_2H_5$	170–172	82
5j	H	Cl	H	$-CH_3$	162–164	80
5k	H	H	Cl	$-C_2H_5$	173–175	83
5l	H	H	Cl	$-CH_3$	159–161	81

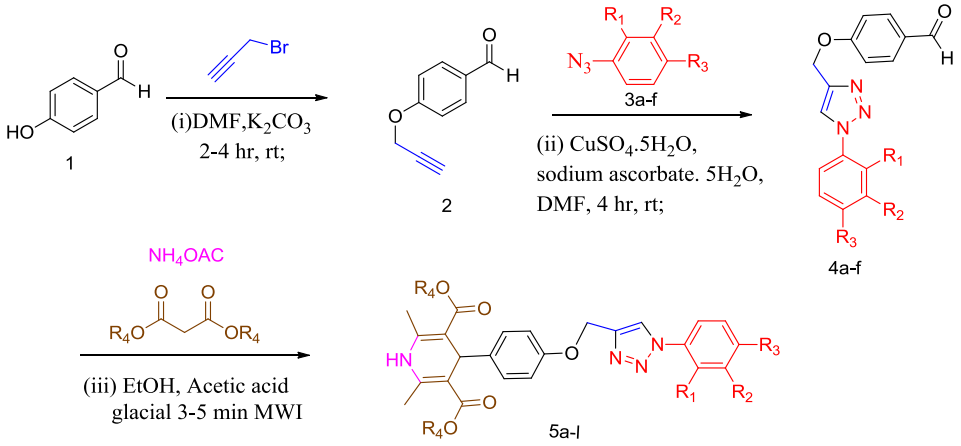

Scheme 1. Alkyl substituted 4-(4-(1-(3-acetylphenyl)-1H-1, 2, 3-triazole-4yl) methoxy) phenyl)-2,6-dimethyl-1,4-dihydropyridine-3,5-dicarboxylates (**5a-l**).

Table 2
Inhibition of α-Glucosidase activity of novel 4-(1-aryl-1*H*-1, 2, 3-triazol-4-yl)-1,4-dihydropyridine derivatives (5a-l).

Compound	R^1	R^2	R^3	R^4	IC_{50} (μM ± SEM)
5a	H	H	H	C_2H_5	201.45 ± 2.56
5b	H	H	H	CH_3	225.92 ± 1.06
5c	H	OCH_3	H	C_2H_5	283.41 ± 2.31
5d	H	OCH_3	H	CH_3	174.99 ± 2.57
5e	H	H	CH_3	C_2H_5	136.87 ± 1.53
5f	H	H	CH_3	CH_3	124.95 ± 1.48
5g	H	$COCH_3$	H	C_2H_5	72.71 ± 1.09
5h	H	$COCH_3$	H	CH_3	73.83 ± 1.17
5i	H	Cl	H	C_2H_5	85.96 ± 1.84
5j	H	Cl	H	CH_3	121.60 ± 2.13
5k	H	H	Cl	C_2H_5	130.68 ± 1.51
5l	H	H	Cl	CH_3	128.71 ± 2.04
Acarbose	–	–	–	_	395.17 ± 1.07

Table 3
% inhibition of α-Glucosidase activity of novel 4-(1-aryl-1*H*-1, 2, 3-triazol-4-yl)-1,4-dihydropyridine derivatives (5a-l).

Sample Used	% inhibition of α-glucosidase activity
Acarbose	98.7
5a	62.4
5b	58.6
5c	55.3
5d	68.3
5e	59.6
5f	67.2
5g	98.3
5h	97.5
5i	96.8
5j	66.4
5k	63.7
5l	60.9

Table 4
Dock score of synthesized molecules **5a-l** from Glide Docking**: 1Y5M.**

Compound	Docking score	XP G score	H bond
5a.	−6.3	−6.3	−0.459
5b	−6.655	−6.655	−0.118
5c	−3.981	−3.981	−0.7
5d	−6.475	−6.475	−0.43
5e	−4.273	−4.273	−0.7
5f	−5.386	−5.386	−0.7
5 g	−9.758	−9.758	0
5 h	−8.495	−8.495	−0.7
5i	−6.306	−6.306	0
5 J	−7.929	−7.929	−0.7
5 k	−2.642	−2.642	−0.201
5l	−7.634	−7.634	−0.396
Rosiglitasone	−7.248	−8.197	−1.691

quantified binding energies were −8.6 kcal mol^{-1} for 5 g and −8.9 kcalmol^{-1} for 5 h, respectively, which were in good agreement with the results obtained from the *in vitro* 11β -HSD1 assay. It was concluded that, the molecular docking analysis provided a key understanding of significant interactions to explain the detailed molecular mechanisms when 5g and 5h bind with 11β -HSD1 for their further development of 11β -HSD1 inhibitors.

2.2.4. In-vivo anti-diabetic activity

The *in-vivo* anti-diabetic activity of 4-(1-aryl-1*H*-1, 2, 3-triazol-4-yl)-1,4-dihydropyridine derivatives (5a-l) were tested for hypoglycaemic activity using alloxan-treated male albino mice. Out of all the compounds tested, it was obvious that the *meta* substituted 1,4-dihydropyridine 1,2,3-triazole hybrid derivatives **5g, 5h, 5i, and 5j** possess

Table 5
The hypoglycaemic activity of novel 4-(1-aryl-1*H*-1, 2, 3-triazol-4-yl)-1,4-dihydropyridine derivatives (5a-l).

Compound	Reduction in plasma glucose level, %	p
5a.	6	0.05
5b	7	0.05
5c	2	0.05
5d	7	0.05
5e	3	0.05
5f	4	0.05
5g	23	< 0.01*
5h	22	< 0.01*
5i	14	< 0.01*
5j	17	< 0.01*
5k	3	0.05
5l	16	< 0.01*
Rosiglitasone	21	< 0.01*

* Compounds 5g, 5h, 5i, 5j and 5k were showed significant reduction of plasma glucose levels, compared with Rosiglitasone.

marked hypoglycaemic activity. The efficiency of these compounds is more than that of Rosiglitasone, probably due to meta substitution of acetyl group in 5g, 5h and chloro group in 5i, 5j. But methoxy substituted molecules have not exhibited significant hypoglycaemic activity like activity reported molecules. As a whole *meta*-acetyl, meta-chloro, and para chloro substituted compounds are reported for increase in the hypoglycemic activity. Glucose was determined by the micro colorimetric copper reduction technique of Strookman and Hazelwood. Results are expressed as % reduction of the plasma glucose levels compared to the control value. Statistical significance was assessed by Student's T-test. Statistical significance was accepted wherever the calculated *T*-value exceeded the tabulated *T*-value at the p = 0.05 level.

3. Conclusion

In conclusion, we have synthesized a novel series of 1,4-dihydropyridine based 1,2,3-triazole moieties by using click chemistry followed by multi component reaction (MCR) starting from 4-hydroxy benzaldehyde. All the synthesized compounds were confirmed by ^{1}H NMR, ^{13}C NMR, IR and mass spectrometry. *In-vitro* antidiabetic activity evaluations showed that most of the synthesized 1, 4-dihydropyridine −1, 2, 3-triazole hybrids exhibited good to excellent activity. These results clearly showed that 1,4-dihydropyridine −1,2,3-triazole motifs have biological activity. Addition optimizations of these identified compounds as well as structural modifications are in progress in order to enhance the efficacy against the above activities. To know the mechanism of action of these compounds, the most potent compounds (5g and 5h) were further studied by testing its 11-Beta-Hydroxysteroid dehydrogenase-1 inhibitory activity through *in vitro* enzymatic experiments. Results showed that the 11β-HSD1 inhibitory activity of compounds **5g** and **5h** was stable and efficient. In addition the mechanism of action of **5g** and **5h** were validated by performing molecular docking analysis. Molecular docking studies show ligand to target interactions and ligand potential towards receptor which generated dock scores, electrostatic energies between the desired molecular complex and hydrogen bond interactions (both side and back chain). Twelve ligand molecules were identified for docking studies against the target 1y5m. The ligands with favorable docking scores and significant glide energy values with good binding affinities have been studied further. Four bioactive molecules were found to have efficient docking scores with good binding affinities compared to Rosiglitasone. In general, the docking is mediated by much van-der Wall forces, electrostatic energy, and inter-atomic interactions. Moreover, these binding affinities also strongly rely on contributions to other factors such as entropy, desolvation, and flexibility of receptor molecule.

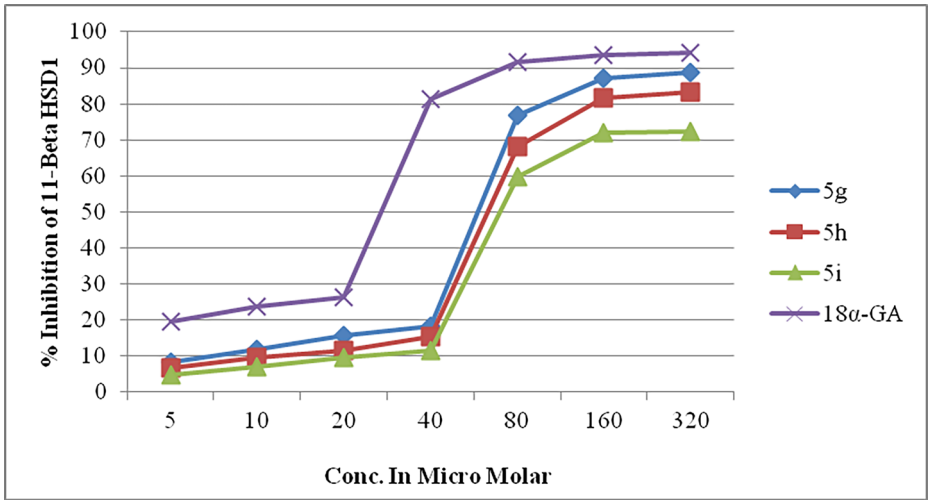

Graph 1. % inhibition of 11β-HSD1 on treatment with novel 5g, 5h, and 5i.

4. Experimental

4.1. General experimental methods

All the reactions were performed in oven-dried apparatus. Reactions were monitored by thin layer chromatography (TLC) on silica gel plates (60 F_{254}), visualizing with ultraviolet light/iodine vapors. Column chromatography was performed on silica gel (60–120 mesh) using distilled hexane and ethyl acetate. ^{1}H NMR and ^{13}C NMR spectra were determined in $CDCl_3$ or DMSO by using 400 and 100 MHz spectrometers (Instrument Bruker Avance II 400 MHz). Mass spectra were recorded on QSTAR XL GCMS mass spectrometer. Infrared spectra were recorded on a Shimadzu FT-IR-8400 s spectrometer. Melting points were determined in open glass capillary tubes on a Gallen-Kamp MFB-595 apparatus and were uncorrected.

4.2. General procedure for the preparation of 4-((1-aryl-1H-1, 2, 3 triazol-4-yl)methoxy) benzaldehydes (4a-f)

The synthesis of above compounds **(4a-f)** were started with 4-hydroxy benzaldehyde **(1).** It was propargylated by propargyl bromide in dry DMF and dry K_2CO_3 25–30 °C under stirring affording the O-propargylated benzaldehyde **(2)** in high yields. The O-propargylated benzaldehyde **(2)** was reacted with different aryl azides **(3a-f)** using Click chemistry in $CuSO_4{\cdot}5H_2O$ with sodium ascorbate to form 1, 2, 3-triazole contain its benzaldehydes **(4a-f)** [28].

4.3. General procedure for the preparation of diethyl 4-(4-(1-(3-acetylphenyl)-1H-1,2,3-triazole-4yl)methoxy)phenyl)-2,6-dimethyl-1,4-dihydropyridine-3,5-dicarboxylate (5a-l)

The synthetic route for title compounds **(5a-l)** was performed using two different techniques (Scheme 1):

a. Conventional method:

The synthesis of compounds **(5a-l)** (Scheme 1):To the mixture of 4-((1-aryl-1H-1,2,3-triazol-4-yl) methoxy) benzaldehydes **(4a-f)** (0.1 gm) (0.1 mmol), ethyl acetoacetate or methyl acetoacetate (0.093 gm) (0.2 mmol) and ammonium acetate (0.22gm) (0.8 mmol) in ethanol 5 ml in a 100 ml round bottomed flask was added catalytic amounts of acetic acid. The reaction was attaché to a reflux condenser and refluxed

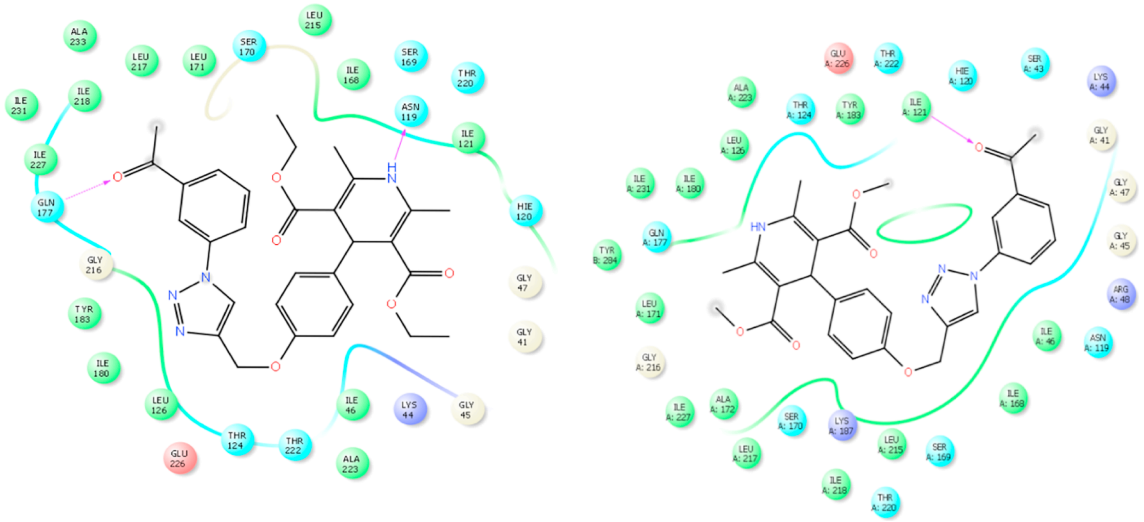

Fig. 2. 2D diagrams of best-fit molecules (a) 5 g and (b) 5 h showing ligand interaction with different amino acid residues of the protein 11βeta-HSD1 (PDB ID: 1Y5M).

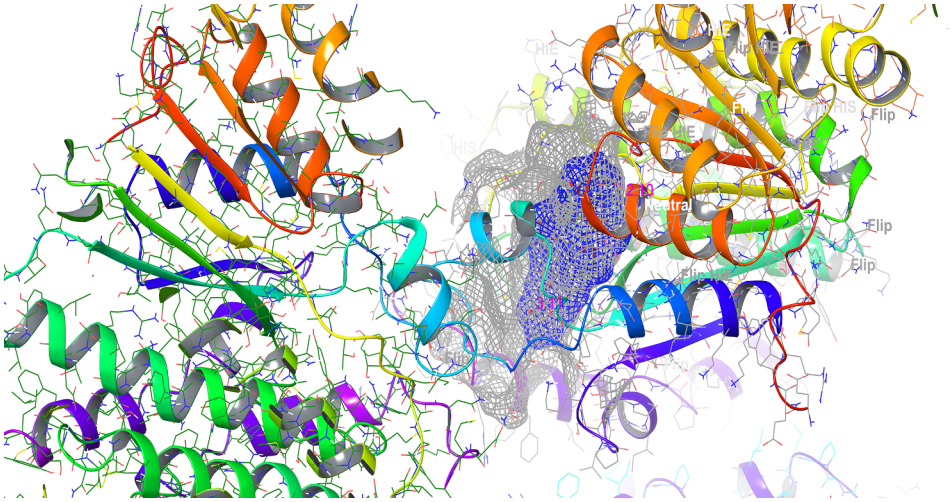

Fig. 3. 3D image of the top molecule 5g (mesh) in the active site pocket of the protein 11βeta-HSD1 (ribbon representation).

at 80 °C for 2–3 h. The progress of the reaction was monitored by TLC. Upon completion the contents of the flask was cooled to room temperature and poured into a 100 ml beaker containing crushed ice. Solids at the bottom were filtered through a Buchner funnel and dried in vacuum at reduced pressure to yield crude compounds which were purified by column chromatography using hexane/ethyl acetate (1:3 v/v) to afford 4-((4-(4,5-diphenyl-1H-imidazole-2-yl)phenoxy)methyl)-1-aryl-1H-1,2,3-triazoles (5a-l) gave excellent yields 55–63%.

b. Microwave method:

The synthesis of compounds **(5a-l)** (Scheme 1):To a mixture of 4-((1-aryl-1H-1,2,3-triazol-4-yl) methoxy) benzaldehydes **(4a-f)** (0.1 gm) (0.1 mmol), ethyl acetoacetate or methyl acetoacetate (0.093 gm) (0.2 mmol) and ammonium acetate (0.22gm) (0.8 mmol) in ethanol 5 ml in a 100 ml beaker was added catalytic amounts of acetic acid were added and treated under microwave irradiation at 180 W for 3–5 min. The progress of the reaction was monitored by TLC at regular intervals of 20 sec. After the completion of the reaction, the contents of the beaker was cooled to room temperature and poured into a 100 ml beaker containing crushed ice. Solids at the bottom were filtered through a Buchner funnel and dried in vacuum at reduced pressure to yield crude compounds which were purified by column chromatography using hexane/ethyl acetate (1:3 v/v) to afford 4-((4-(4,5-diphenyl-1H-imidazole-2-yl)phenoxy)methyl)-1-aryl-1H-1,2,3-triazoles (5a-l) in yields of 80–89%. Comparison of the result obtained under conventional heating method and microwave irradiation are presented in Table 6.

Table 6
Conventional heating and microwave irradiation optimization for the synthesis of compounds **5a-l.**

Compound Number	Conventional heating (A)		Microwave irradiation (B)	
	Time (h)	Yield (%)	Time (min)	Yield (%)
5a	2	61	3	87
5b	2	62	5	85
5c	3	63	3	89
5d	2	60	4	87
5e	3	58	4	84
5f	3	59	5	83
5g	2	58	4	87
5h	2	59	3	85
5i	3	57	4	82
5j	3	55	5	80
5k	2	60	4	83
5l	3	61	3	81

4.4. In-vitro antidiabetic activity

4.4.1. α-Glucosidase inhibitory assay

α-Glucosidase inhibitory activity was assayed by using 0.1 M phosphate buffer (pH 6.8) at 37 °C. The enzyme (0.1 U/mL) in phosphate buffer saline was incubated with various concentrations of test compounds at 37 °C for 15 min. Then 1.25 mM p-nitrophenyl-D-glucopyranoside was added to the mixture as a substrate. After further incubation at 37 °C for 30 min the absorbance was measured spectrophotometrically at 405 nm. The sample solution was replaced by DMSO as a control. Acarbose was used as a positive control.

4.4.2. In-vitro 11β-hydroxysteroid dehydrogenase assay

Enzymatic activities of 5 g and 5 h against 11β -HSD1 were determined by the scintillation proximity assay (SPA) using microsomes containing 11β-HSD1 according to previous studies [29]. Briefly, the full-length cDNAs of human 11β-HSD1 were isolated from cDNA libraries provided by NIH Mammalian Gene Collection and cloned into pcDNA3 expression vectors (Invitrogen, Carlsbad, CA, USA) by PCR. HEK-293 cells were transfected with the pcDNA3-derived expression plasmids and selected by cultivation 700 mg/mL. The microsomal fraction over-expressing 11β-HSDs was prepared from the HEK-293 cells stably transfected with 11β-HSDs and used as the enzyme source for SPA. The assay was performed in a 96-well microtitre plate. Compounds (5g, 5h, and 5i) with different concentrations ranging from 5 to 320 μM, were added, followed by adding 80 ml of 50 mM HEPES buffer, pH 7.4 containing 25 nM cortisone [1,2-^{3}H(N)] (Amersham, Buck inghamshire, UK) and 1.25 mM NADPH (for 11β-HSD1 assay). 18α-glycyrrhetinic acid was used as a selective inhibitor of human 11β-HSD1.

4.4.3. In-vivo antidiabetic activity

Compounds (5a-l) were tested for hypoglycaemic activity using alloxan-treated male albino mice of 20–23 g body weight. 100 mg/kg of Alloxan was injected into the tail vein at a concentration of 10 mg/ml dissolved in isotonic solution (normal saline). Three days later, the mice were given the test compounds orally in suspension in carboxymethyl cellulose (CMC) solution at a concentration of 0.2 mmol/kg body weight. Each day, a group of 4 albino mice were used as a control group and one group of 5 albino mice was given 100 mg of Rosiglitasone/kg. Up to 6 groups of 4 albino mice received the test compounds. Blood samples were collected into 0.04% NaF solution at 0, 1 and 3 h.

4.5. SAR studies

All the 12 compounds prepared contained the triazole pharmacophore and the 1,4-dihydropyridine-3,5-dicarboxylate moiety with a –OCH_2– linker. The N1 protonation of 1, 4-DHP shows changes in hydrogen bonding in different derivatives and is a hydrogen bond donor. The presence of C-3 and C-5 position ester groups is known to be responsible for the optimum activity and for distinguishing antagonistic and agonistic activity [30]. The perpendicular confirmation (enantiomeric selectivity) of 1,4-DHPs has been proposed to be essential for the activity. The phenyl triazole with different substituents at the 4th position was significant than other positions [31]. Some amino acids are required to maintain the integrity of the interaction site and are not directly involved in the interaction [32]. Based on the observations the synthesized compounds were analyzed. For the **5a** and **5b** derivatives, the replacement of the ethyl group with a methyl group at the R_4 position shows a decrease in the activity as evident from Mol dock score, IC_{50} value and % inhibition of glutamate activity. This may be due to the strong pi-alkyl interaction with Ala172 as seen only in **5a**. Upon substitution of R_2 (meta) position with methoxy group and R_4 position with methyl group the activity increased due to hydrogen bonding of the methoxy group with Thr124 in **5d**. Generally, the position of the OMe group in the phenyl ring also plays an important role in the activity (2-OMe > 3-OMe > 4-OMe). Among **5e** and **5f** the methyl substitution at R_3 position (stable) has shown greater activity for **5e** due to strong pi-sigma, pi-alkyl, pi-amide interactions and hydrogen bonding with Tyr183. For compounds **5g**, methyl ketone (acyl group) substitution at R_2 position results in hydrogen bonding with acetyl group and Gly177. There was also an additional hydrogen bond between Asn119 and an electronegative atom (Nitrogen) that results in enhanced activity. This compound has shown a top Mol dock score and higher percentage inhibition along with the lower IC_{50} value (72.71 ± 1.09) than standard Acarbose with 395.17 ± 1.07. In the case of **5h,** it has a hydrogen bond between Ile121 and an acetyl group moiety. In **5i** and **5j**, substitution at R_2 position with a chloro electron withdrawing group showed greater activity due to strong, pi-alkyl, van der Waals and hydrogen bond interactions. Between **5k** and **5l**, the chloro substitution at the *para* position shows pi interaction with the chloro group in **5l** and has greater activity than **5k**. Electron withdrawing compounds *ortho* or *meta* substitutions of triazole attached phenoxy group possess optimum activity, while para-substitution shows decrease in activity according to its electronic and steric effects. Compounds **5i** and **5j** showed better activity than **5k** and **5l**. The highest effective compounds were found to be **5g**, **5h** along with moderate activity for **5a, 5d, 5e, 5f, 5i, 5j, 5k, 5l** and least activity for **5b** and **5c**. The derivatives with chloro and hydroxyl groups showed maximum activity in comparison to those with a methyl group, which in turn were more reactive than the methoxy derivatives. Thus, this association reveals that activity is influenced by the nature of the substitution.

4.6. Spectral data

4.6.1. Diethyl 2,6-dimethyl-4-(4-((1-phenyl-1H-1, 2, 3-triazol-4-yl) methoxy) phenyl) −1, 4-dihydropyridine −3, 5-dicarboxylate (5a)

Yield 87%, mp: 165–168 °C; Rf = 0.40 (EtOAc:*n*-Hexane 2:3); IR (KBr, cm^{-1}): 3218, 3089, 2937, 1685, 1501.^{1}H NMR (400 MHz, $CDCl_3$) δ ppm 8.03 (s, 1H), 7.76 (d, *J* = 8.6 Hz 2H), 7.56–7.51 (m, 2H), 7.45 (t, *J* = 7.4 Hz, 1H), 7.21 (d, *J* = 8.7 Hz, 2H), 6.86 (d, *J* = 8.7 Hz, 2H), 5.25 (s, 2H), 4.93 (s, 1H), 4.08 (m, 4H), 2.33 (s, 6H)) 0.89 (s, 6H)). ^{13}C NMR (100 MHz, $CDCl_3$) δ ppm 167.6, 156.5, 143.6, 141.0, 138.5, 136.6, 129.7, 129.7, 120.6, 114.0, 104.3, 62.0, 59.7, 38.8, 31.9, 22.6, 19.6, 14.2. LC-MS *m/z* at 503 [M + H] +; Elemental analysis calculated for: $C_{28}H_{30}N_4O_5$: C, 66.92; H, 6.02; N, 11.15; Found: C, 66.89; H, 5.98; N, 11.13.

4.6.2. Dimethyl 2,6-dimethyl-4-(4-((1-phenyl-1H-1,2,3-triazol-4-yl) methoxy)phenyl)-1,4-dihydropyridine-3,5-dicarboxylate (5b)

Yield 85%, mp: 156–158 °C; Rf = 0.40 (EtOAc:*n*-Hexane 2:3); IR (KBr cm^{-1}): 3221, 3090, 2943, 1689, 1504. ^{1}H NMR (400 MHz, $CDCl_3$) δ ppm 8.09 (s, 1H), 7.75 (d, *J* = 8.3, 2H), 7.60–7.51 (m, 4H), 7.46 (t, *J* = 7.4, Hz, 1H), 7.20 (d, *J* = 8.7 Hz, 5H), 7.13–7.04 (m, 23H), 6.87 (d, *J* = 8.7 Hz, 5H), 5.35 (s, 2H), 5.26 (s 1H), 3.97 (s, 6H), 2.59 (s, 6H). ^{13}C NMR (100 MHz, $CDCl_3$) δppm 168.8, 155.6, 153.3, 144.7, 143.0, 132.7, 129.8, 128.9, 126.6, 120.6, 114.8, 100.7, 62.1, 52.5, 29.7, 23.2, 17.0. LC-MS *m/z* at 475 [M + H] +; Elemental analysis calculated for: $C_{26}H_{26}N_4O_5$: C, 65.81; H, 5.52; N, 11.81; Found: C, 65.79; H, 5.50; N, 11.79.

4.6.3. Diethyl 4-(4-((1-(2-methoxyphenyl)-1H-1,2,3-triazol-4-yl)methoxy) phenyl)-2,-dimethyl-1,4-dihydropyridine-3,5-dicarboxylate (5c)

Yield 89%,mp:148–150 °C; Rf = 0.43(EtOAc:nHexane2:3);IR (KBrcm^1): 3217, 3088, 2945, 1689, 1500, 1217. ^{1}H NMR (400 MHz, $CDCl_3$) δ ppm 8.15 (s, 1H), 7.78 (d, *J* = 7.8 Hz, 1H), 7.42 (t, *J* = 7.3 Hz, 1H), 7.21 (d, *J* = 8.6 Hz, 2H), 7.10 (dd, *J* = 12.9, 7.9 Hz, 2H), 6.88 (d, *J* = 8.6 Hz, 2H), 5.25 (s, 2H), 4.93 (s, 1H), 4.13–4.03 (m, 4H), 3.88 (s, 3H), 2.33 (s, 6H), 1.22 (t, *J* = 7.1 Hz, 6H). ^{13}C NMR (100 MHz, $CDCl_3$) δppm 167.6, 156.5, 145.1, 143.7, 141.1, 138.9, 134.7, 130.2, 129.1, 120.8, 120.5, 114.0, 104.2, 62.0, 59.6, 38.8, 21.0, 19.5, 14.2. LC-MS *m/z* at 533 [M + H] +; Elemental analysis calculated for: $C_{29}H_{32}N_4O_6$: C, 65.40; H, 6.06; N, 10.52; Found: C, 65.39; H, 6.02; N, 10.47.

4.6.4. Dimethyl 4-(4-((1-(2-methoxyphenyl)-1H-1,2,3-triazol-4-yl) methoxy)phenyl)-2,6-dimethyl-1,4-dihydropyridine-3,5-dicarboxylate (5d)

Yield 87%,mp:140–142 °C; Rf = 0.43(EtOAc:n-Hexane2:3);IR(KBr cm^1): 3221, 3093, 2980, 1687, 1500, 1217. ^{1}H NMR (400 MHz, $CDCl_3$) δ ppm 8.15 (s, 1H), 7.77 (d, *J* = 7.9, 1H), 7.52 (t, *J* = 7.3 Hz, 1H), 7.19 (d, *J* = 8.6 Hz, 2H), 7.10 (dd, *J* = 12.5, 8.0 Hz, 2H), 6.89 (d, *J* = 8.6 Hz, 2H), 5.29 (s, 2H), 4.94 (s, 1H), 3.89 (s, 3H), 3.64 (s, 6H), 2.33 (s, 6H). ^{13}C NMR (100 MHz, $CDCl_3$) δppm 168.0, 156.6, 154.2, 145.1, 145.0, 138.9, 130.2, 128.7, 120.8, 120.5, 114.2, 104.1, 62.1, 50.9, 38.4, 21.0, 19.6. LC-MS *m/z* at 504 [M + H] +; Elemental analysis calculated for: $C_{27}H_{28}N_4O_6$: C, 64.27; H, 5.59; N, 11.10; Found: C, 64.24; H, 5.56; N, 11.07.

4.6.5. Diethyl 2,6-dimethyl-4-(4-((1-(p-tolyl)-1H-1,2,3-triazol-4-yl) methoxy)phenyl)-1,4-dihydropyridine-3,5-dicarboxylate (5e)

Yield 84%, mp: 142–144 °C; Rf = 0.5 (EtOAc:*n*-Hexane 2:3); IR (KBr cm^1):3224, 3095, 2947, 1693, 1500, 1217. ^{1}H NMR (400 MHz, $CDCl_3$) δ ppm 7.98 (s, 1H), 7.60 (d, *J* = 8.4 Hz, 2H), 7.31 (d, *J* = 8.2 Hz, 2H), 7.21 (d, *J* = 8.7 Hz, 2H), 6.86 (d, *J* = 8.7 Hz, 2H), 5.24 (s, 2H), 4.93 (s, 1H), 4.16–4.01 (m, 4H), 2.42 (s, 3H), 2.32 (s, 6H), 1.22 (t, *J* = 7.1 Hz, 6H). ^{13}C NMR (100 MHz, $CDCl_3$) δ ppm 167.6, 156.7, 151.1, 143.8, 143.6, 140.9, 130.1, 129.0, 126.2, 125.5, 124.9, 121.2, 112.2, 104.3, 62.0, 59.6, 55.9, 38.7, 19.5, 14.2. LC-MS *m/z* at 547 [M + H] +; Elemental analysis calculated for: $C_{30}H_{34}N_4O_6$: C, 65.92; H, 6.27; N, 10.25; Found: C, 65.89; H, 6.25; N, 10.21.

4.6.6. Dimethyl 2,6-dimethyl-4-(4-((1-(p-tolyl)-1H-1,2,3-triazol-4-yl) methoxy)phenyl)-1,4-dihydropyridine-3,5-dicarboxylate (5f)

Yield 83%,mp:135–137 °C; Rf = 0.5 (EtOAc:n-Hexane2:3);IR (KBr cm^1): 3226, 3097, 2981, 1681, 1498, 1217. ^{1}H NMR (400 MHz, $CDCl_3$) δ ppm 7.98 (s, 1H), 7.61 (d, *J* = 8.1 Hz, 2H), 7.31 (d, *J* = 8.2 Hz, 2H), 7.20 (d, *J* = 8.5 Hz, 2H), 6.87 (d, *J* = 8.4 Hz, 2H), 5.24 (s, 2H), 4.95 (s, 1H), 3.65 (s, 6H), 2.42 (s, 3H), 2.34 (s, 6H). ^{13}C NMR (100 MHz, $CDCl_3$) δ ppm 168.0, 156.7,151.1, 144.0, 143.7, 140.5, 130.1, 128.6, 126.2, 125.5, 125.0, 121.2, 114.3, 112.2, 104.1, 62.0, 55.9, 50.9, 38.4, 19.5 LC-MS *m/z* at 519 [M + H] +; Elemental analysis calculated for: $C_{28}H_{30}N_4O_6$: C, 64.85; H, 5.83; N, 10.80; Found: C, 64.82; H, 5.81; N, 10.79.

4.6.7. Diethyl 4-(4-((1-(3-acetylphenyl)-1H-1,2,3-triazol-4-yl)methoxy) phenyl)-2,6-dimethyl-1,4-dihydropyridine-3,5-dicarboxylate (5g)

Yield 87%, mp: 162–164 °C; Rf = 0.5 (EtOAc:*n*-Hexane 2:3); IR (KBr cm^1):3221, 3092, 2949, 1691, 1500, 1215. ^{1}H NMR (400 MHz, $CDCl_3$) δ ppm 8.30 (s, 1H), 8.12 (s, 1H), 8.05–7.98 (m, 2H), 7.65 (t, *J* = 7.9 Hz, 1H), 7.22 (d, *J* = 8.7 Hz, 2H), 6.86 (d, *J* = 8.7 Hz, 2H), 5.26 (s, 2H), 4.94 (s, 1H), 4.16–4.03 (m, 4H), 2.68 (s, 3H), 2.33 (s, 6H), 1.22 (t, *J* = 7.1 Hz, 6H). ^{13}C NMR (100 MHz, $CDCl_3$) δ ppm 196.6, 167.6, 156.4, 145.7, 143.5, 141.1, 138.5, 137.4, 130.2, 129.1, 128.4, 124.8, 120.7, 119.8, 114.0, 104.3, 61.9, 59.7, 38.8, 26.7, 19.6, 14.2. LC-MS *m/z* at 545 [M + H] +; Elemental analysis calculated for: C, 66.16; H, 5.92; N, 10.29; Found: C, 66.11; H, 5.88; N, 10.26.

4.6.8. Dimethyl 4-(4-((1-(3-acetylphenyl)-1H-1,2,3-triazol-4-yl)methoxy) phenyl)-2,6-dimethyl-1,4-dihydropyridine-3,5-dicarboxylate (5h)

Yield 85%,mp:151–153 °C; Rf = 0.5 (EtOAc:n-Hexane2:3);IR (KBr cm^1): 3223, 3093, 2983, 1689, 1500, 1215. ^{1}H NMR (400 MHz, $CDCl_3$) δ ppm 8.30 (s, 1H), 8.12 (s, 1H), 8.02 (d, *J* = 7.8 Hz, 2H), 7.66 (t, *J* = 8.0 Hz, 1H), 7.20 (d, *J* = 8.5 Hz, 2H), 6.87 (d, *J* = 8.5 Hz, 2H), 5.27 (s, 2H), 4.95 (s, 1H), 3.65 (s, 6H), 2.68 (s, 3H), 2.34 (s, 6H) ^{13}C NMR (100 MHz, $CDCl_3$) δ ppm196.6,168.0, 156.5, 145.7, 143.9, 140.7, 138.5, 137.4, 130.2, 128.7, 128.4, 124.8, 120.7, 119.8, 104.0, 61.9, 50.9, 38.4, 26.7, 19.6. LC-MS *m/z* at 517 [M + H] +; Elemental analysis calculated for $C_{28}H_{28}N_4O_6$: C, 65.11; H, 5.46; N, 10.85; Found: C, 65.07; H, 5.39; N, 10.86.

4.6.9. Diethyl 4-(4-((1-(3-chlorophenyl)-1H-1,2,3-triazol-4-yl)methoxy) phenyl)-2,6-dimethyl-1,4-dihydropyridine-3,5-dicarboxylate (5i)

Yield 82%,mp:170–172 °C; Rf = 0.40 (EtOAc:n-Hexane2:3);IR(KBr cm^1): 3224, 3095, 2985, 1685, 1500, 1217.^{1}H NMR (400 MHz, $CDCl_3$) δ ppm 8.02 (s, 1H), 7.79 (t, *J* = 2.0 Hz, 1H), 7.67 (d, *J* = 7.6 Hz, 1H), 7.43 (tt, *J* = 4.7, 3.2 Hz, 2H), 7.23 (d, *J* = 8.5 Hz, 2H), 6.88 (d, *J* = 8.5 Hz, 2H), 5.25 (s, 2H), 4.94 (s, 1H), 4.14–4.03 (m, 4H), 2.33 (s, 6H), 1.22 (t, *J* = 7.1 Hz, 6H). ^{13}C NMR (100 MHz, $CDCl_3$) δ ppm 167.6, 156.4, 145.6, 143.6, 141.1, 137.8, 135.6, 130.8, 129.1, 128.9, 120.8, 118.5, 114.0, 104.3, 61.9, 59.7, 38.8, 19.5, 14.2. LC-MS *m/z* at 537 [M + H] +; Elemental analysis calculated for $C_{28}H_{29Cl}N_4O_5$: C, 62.62; H, 5.44; N, 10.85; Found: C, 62.60; H, 5.39; N, 10.83.

4.6.10. Dimethyl 4-(4-((1-(3-chlorophenyl)-1H-1,2,3-triazol-4-yl)methoxy) phenyl)-2,6-dimethyl-1,4-dihydropyridine-3,5-dicarboxylate (5j)

Yield 80%,mp:162–164 °C; Rf = 0.40 (EtOAc:n-Hexane2:3);IR(KBr cm^1): 3224, 3095, 2980, 1689, 1500, 1215. ^{1}H NMR (400 MHz, $CDCl_3$) δ ppm 8.02 (s, 1H), 7.79 (s, 1H), 7.64 (d, *J* = 7.6 Hz, 1H), 7.50–7.37 (m, 2H), 7.20 (d, *J* = 8.5 Hz, 2H), 6.86 (d, *J* = 8.5 Hz, 2H), 5.25 (s, 2H), 4.95 (s, 1H), 3.64 (s, 6H), 2.30 (s, 6H).). ^{13}C NMR (100 MHz, $CDCl_3$) δ ppm 168.0, 156.5, 145.6, 144.0, 140.7, 137.8, 135.6, 130.8, 128.7, 120.8, 118.5, 114.2, 104.0, 61.9, 51.0, 38.4, 19.5 LC-MS *m/z* at 510 [M + H] +; Elemental analysis calculated for $C_{26}H_{25Cl}N_4O_5$: C, 61.36; H, 4.95; N, 11.01; Found: C, 61.33; H, 4.93; N, 10.93.

4.6.11. Diethyl 4-(4-((1-(4-chlorophenyl)-1H-1,2,3-triazol-4-yl)methoxy) phenyl)-2,6-dimethyl-1,4-dihydropyridine-3,5-dicarboxylate (5k)

Yield 83%, mp: 173–175 °C; Rf = 0.40 (EtOAc:*n*-Hexane 2:3); IR (KBr cm^1): 3221, 3093, 2983, 1687, 1503.^{1}H NMR (400 MHz, $CDCl_3$) δ ppm 8.01 (s, 1H), 7.72 (d, *J* = 8.8, Hz, 2H), 7.53–7.46 (d, *J* = 8.8, Hz, 2H), 7.21 (d, *J* = 9.2, Hz, 2H), 6.85 (d, *J* = 8.7 Hz, 2H), 5.25 (s, 2H), 4.93 (s, 1H), 4.14–4.04 (m, 4H), 2.33 (s, 6H), 1.24 (t, *J* = 7.1 Hz, 6H). ^{13}C NMR (100 MHz, $CDCl_3$) δppm 167.6, 156.4, 145.6, 143.6, 141.1, 134.6, 129.9, 121.7, 120.7, 104.3, 62.0, 159.7, 38.8, 29.6, 19.6, 14.2. LC-MS *m/z* at 538 [M + H] +; Elemental analysis calculated for $C_{28}H_{29}ClN_4O_5$: C, 62.62; H, 5.44; N, 10.43; Found: C, 62.59; H, 5.42; N, 10.40.

4.6.12. Dimethyl 4-(4-((1-(4-chlorophenyl)-1H-1,2,3-triazol-4-yl)methoxy) phenyl)-2,6-dimethyl-1,4-dihydropyridine-3,5-dicarboxylate (5l)

Yield 81%, mp: 159–161 °C; Rf = 0.40 (EtOAc:*n*-Hexane 2:3); IR (KBr cm^1): 3219, 3090, 2979, 1688, 1501. ^{1}H NMR (400 MHz, $CDCl_3$) δ ppm 8.01 (s, 1H), 7.69 (d, *J* = 8.8 Hz, 2H), 7.50 (d, *J* = 8.8 Hz, 2H), 7.20 (d, *J* = 8.6 Hz, 2H), 6.86 (d, *J* = 8.7 Hz, 2H), 5.25 (s, 2H), 4.95 (s, 1H), 3.65 (s, 6H), 2.33 (s, 6H). ^{13}C NMR (100 MHz, $CDCl_3$) δ ppm 168.0, 156.5, 143.9, 140.7, 134.6, 129.9, 128.7, 121.7, 120.7, 114.0, 61.9, 51.0, 38.4, 29.6, 22.6, 19.6. LC-MS *m/z* at 509 [M + H] +; Elemental analysis calculated for $C_{26}H_{25}ClN_4O_5$: C, 61.36; H, 4.95; N, 11.01; Found: C, 61.33; H, 4.92; N, 10.98.

Acknowledgements

The authors are thankful to the Head, Department of chemistry, Osmania University, Hyderabad for providing laboratory facilities. E Praveen Kumar is thankful to CSIR-UGC for financial assistance in the form of fellowship and one of the authors NJPS is thankful to OU-DST PURSE-II/60/2017-18, India for financial assistance. We thank the CFRD analytical team for providing spectral analytical facilities.

Appendix A. Supplementary material

Supplementary data to this article can be found online at https://doi.org/10.1016/j.bioorg.2019.103056.

References

[1] E.D. Rosen, B.M. Spiegelman, Adipocytes as regulators of energy balance and glucose homeostasis, Nature 444 (2006) 847–853.
[2] A. Guilherme, J.V. Virbasius, V. Puri, M.P. Czech, Adipocyte dysfunctions linking obesity to insulin resistance and type 2 diabetes, Nat. Rev. Mol. Cell Biol. 9 (2008) 367–377.
[3] C. Beauregard, G. Dickstein, A. Lacroix, Classic and recent etiologies of Cushing's syndrome: diagnosis and therapy, Treat Endocrinol. 1 (2002) 79–94.
[4] J.R. Seckl, B.R. Walker, Mini review: 11βeta-hydroxysteroid dehydrogenase type 1- a tissue-specific amplifier of glucocorticoid action, Endocrinology 142 (2001) 1371–1376.
[5] N.M. Morton, Obesity and corticosteroids: 11βeta–hydroxysteroid type 1 as a cause and therapeutic target in metabolic disease, MolCell Endocrinol. 316 (2010) 154–164.
[6] H. Masuzaki, J. Paterson, H. Shinyama, N.M. Morton, J.J. Mullins, Seckl, et al., A transgenic model of visceral obesity and the metabolic syndrome, Science 294 (2001) 2166–2170.
[7] H. Masuzaki, H. Yamamoto, C.J. Kenyon, J.K. Elmquist, N.M. Morton, J.M. Paterson, et al., Transgenic amplification of glucocorticoid action in adipose tissue causes high blood pressure in mice, J. Clin. Invest. 112 (2003) 83–90.
[8] J.M. Paterson, Metabolic syndrome without obesity: Hepatic overexpression of 11-Beta-hydroxysteroid dehydrogenase type 1 in transgenic mice, Proc. Natl. Acad. Sci. USA 101 (2004) 7088–7093.
[9] Y. Kotelevtsev, M.C. Holmes, A. Burchell, P.M. Houston, D. Schmoll, P. Jamieson, et al., 11βeta-hydroxysteroid dehydrogenase type 1 knockout mice show attenuated glucocorticoid-inducible responses and resist hyperglycemia on obesity or stress, Proc. Natl. Acad. Sci. USA 94 (1997) 14924–14929.
[10] N.M. Morton, M.C. Holmes, C. Fievet, B. Staels, A. Tailleux, J.J. Mullins, et al., Improved lipid and lipoprotein profile, hepatic insulin sensitivity, and glucose tolerance in 11βeta-hydroxysteroid dehydrogenase type 1 null mouse, J. Biol. Chem. 276 (2001) 41293–41300.
[11] N.M. Morton, J.M. Paterson, H. Masuzaki, M.C. Holmes, B. Staels, C. Fievet, et al., Novel adipose tissue-mediated resistance to diet-induced visceral obesity in 11βeta-hydroxysteroid dehydrogenase type 1-deficient mice, Diabetes. 53 (2004) 931–938.
[12] Merck Research Laboratories: The Merck Index, 12th ed.; Rahway, NJ, USA, 1996; p. 1121.
[13] G. Hollis, R. Huber, 11βeta-Hydroxysteroid dehydrogenase type 1 inhibition in type 2 diabetes mellitus, Diabetes ObesMetab. 13 (2011) 1–6.
[14] J. Westerbacka, H. Yki-Jarvinen, S. Vehkavaara, A.M. Hakkinen, R. Andrew, D.J. Wake, et al., Body fat distribution and cortisol metabolism in healthy men: enhanced 5beta-reductase and lower cortisol/cortisone metabolite ratios in men with fatty liver, J. Clin. Endocrinol. Metab. 88 (2003) 4924–4931.
[15] S.L. Boström, B. Ljung, S. Mårdh, S. Forsen, E. Thulin, Interaction of the anti-hypertensive drug felodipine with calmodulin, Nature 292 (1981) 777–778.
[16] M. Iwanami, T. Shibanuma, M. Fujimoto, R. Kawai, K. Tamazawa, T. Takenaka, K. Takahashi, M. Murakami, Synthesis of new water-soluble dihydropyridine vasodilators, Chem. Pharm. Bull. 27 (1979) 1426–1440.
[17] J.E. Arrowsmith, S.F. Campbell, P.E. Cross, J.K. Stubbs, R.A. Burges, D.G. Gardiner, K.J. Blackburn, Long-acting dihydropyridine calcium antagonists. 1, 2-alkoxymethyl derivatives incorporating basic substituents, J. Med. Chem. 29 (1986)

1696–1702.
[18] J.L. Harper, C.S. Camerini-Otero, A.H. Li, S.A. Kim, K.A. Jacobson, J.W. Daly, Dihydropyridines as inhibitors of capacitative calcium entry in Leukemic HL-60 cells, Biochem. Pharmacol. 65 (2003) 329–338.
[19] A. Zarghi, H. Sadeghi, A. Fassihi, M. Faizi, A. Shafiee, Synthesis and calcium antagonist activity of 1,4-dihydropyridines containing phenylamino imidazolyl substituents, Farmaco 58 (2003) 1077–1081.
[20] R. Peri, S. Padmanabhan, S. Singh, A. Rutledge, D.J. Triggle, Permanently charged chiral 1,4-dihydropyridines: Molecular probes of L-type calcium channels. Synthesis and pharmacological characterization of methyl (-trimethyl alkyl ammonium) 1, 4-dihydro-2, 6-dimethyl-4-(3-nitrophenyl)-3,5-pyridine dicarboxylate iodide, calcium channel antagonists, J. Med. Chem. 43 (2000) 2906–2914.
[21] B. Berkels, R. Roesen, S. Dhein, U. Fricke, W. Klaus, Dihydropyridine calcium antagonist-induced modulation of endothelial function: A review, Cardiovasc. Drug Rev. 17 (1999) 179–186.
[22] T. Tsuruo, H. Iida, M. Nojiri, S. Tsukagoshi, Y. Sakurai, Circumvention of vincristine and adriamycin resistance in vitro and in vivo by calcium influx blockers, Cancer Res. 43 (1983) 2905–2910.
[23] A. Krauze, S. Germane, O. Eberlin, I. Sturms, V. Klusa, G. Duburs, Derivatives of 3-cyano-6-phenyl-4-(3′-pyridyl)pyridine-2(1H)-thione and their neurotrophic activity, Eur. J. Med. Chem. 34 (1999) 301–310.
[24] X. Zhou, L. Zhang, E. Tseng, E. Scott-Ramsay, J.J. Schentag, R.A. Coburn, M.E. Morris, New 4-aryl-1, 4-dihydropyridines and 4-aryl pyridine as P-glycoprotein inhibitors, Drug Metab. Dispos. 33 (2005) 321–328.
[25] R.W. Chapman, G. Danko, M.I. Siegel, Effect of extra- and intracellular calcium blockers on histamine and antigen-induced bronchospasm in guinea pigs and rats, Pharmacology 29 (1984) 282–291.
[26] W.J. Malaise, P.C.F. Mathias, Stimulation of insulin release by organic calcium-agonist, Diabetologia 28 (1985) 153–156.
[27] P.M. Stewart, J.W. Tomlinson, Selective inhibitors of 11beta-hydroxysteroid dehydrogenase type 1 for patients with metabolic syndrome: is the target liver, fat, or both? Diabetes 58 (1) (2009) 14–15.
[28] (a) S.Z. Ferreira, H.C. Carneiro, H.A. Lara, R.B. Alves, J.M. Resende, H.M. Oliveira, L.M. Silva, D.A. Santos, R.P. Freitas, A.C.S. Med, Chem. Lett. 6 (2015) 271–275;
(b) M. Irfan, B. Aneja, U. Yadava, S.I. Khan, N. Manzoor, C.G. Daniliuc, M. Abid, Eur. J. Med. Chem. 93 (2015) 246–254;
(c) Z. Jiang, J. Gu, C. Wang, S. Wang, N. Liu, Y. Jiang, G. Dong, Y. Wang, Y. Liu, J. Yao, Z. Miao, W. Zhang, C. Sheng, Eur. J. Med. Chem. 82 (2014) 490–497.
[29] Development and Application of a Scintillation Proximity Assay (SPA) for Identification of Selective Inhibitors of 11??-Hydroxysteroid Dehydrogenase Type 1; Assay and Drug Development Technologies 3 (4) (2005) 367–375.
[30] M.A. Shaldam, M.H. Elhamamsy, E.A. Esmat, T.F. El-Moselhy, 1, 4-dihydropyridine calcium channel blockers: homology modeling of the receptor and assessment of structure activity relationship, ISRN Med. Chem (2014).
[31] P. López-Rojas, M. Janeczko, K. Kubiński, Á. Amesty, M. Masłyk, A. Estévez- Braun, Synthesis and antimicrobial activity of 4-substituted 1, 2, 3-triazole- coumarin derivatives, Molecules 23 (1) (2018) 199.
[32] S. Haider, M.S. Alam, H. Hamid, 1, 2, 3-Triazoles: scaffold with medicinal significance, Inflamm. Cell Signal 95 (2014) 1–12.